J. Phys. Chem. A **2005,** *109,* 2107−2112

Protonated Serine Octamer Cluster: Structure Elucidation by Gas-Phase H/D Exchange Reactions[†]

Ulf Mazurek, Orit Geller, and Chava Lifshitz*
Department of Physical Chemistry and The Farkas Center for Light Induced Processes,
The Hebrew University of Jerusalem, Jerusalem 91904, Israel

Melinda A. McFarland
Department of Chemistry and Biochemistry, Florida State University, Tallahassee, Florida 32306-4390

Alan G. Marshall
Department of Chemistry and Biochemistry, Florida State University, Tallahassee, Florida 32306-4390, and
Ion Cyclotron Resonance Program, National High Magnetic Field Laboratory, Florida State University,
1800 East Paul Dirac Drive, Tallahassee, Florida 32310-4005

Bryan G. Reuben
Faculty of Business, Computing and Information Management, London South Bank University,
London SE1 0AA, U.K.

Received: October 26, 2004; In Final Form: December 16, 2004

The H/D exchange kinetics of the protonated serine octamer was investigated by both flow-tube and FT-ICR experiments. The exchange was observed to be bimodal in agreement with previous observations. Quantitative analysis of the experimental results led to site-specific H/D exchange rate constants on the basis of which the structures of both ion populations were deduced. We observe the two separate conformers exchanging 33 hydrogens each—in an independent manner and at different rates. This result was achieved through a probabilistic algorithm that groups together equivalent hydrogen atoms having equal rate constants. The slower exchanging population A is assigned an all-zwitterionic structure. Its faster exchanging counterpart B is assigned an all-neutral structure. Population A was found to be more stable toward collision-induced activation than population B. All of these findings are consistent with previous experimental results, thus comprising a self-consistent picture of the protonated serine octamer and its gas-phase properties.

Introduction

Chirality is a characteristic signature of life on earth; nearly all biological polymers are made from homochiral building blocks. However, the origin of homochirality is not yet understood, thus constituting a research field of great interest in chemistry. Recently, clusters formed from eight serine molecules have gained considerable attention. After being observed as protonated octamers in the gas phase[1] and found to exhibit a remarkable stereoselectivity in forming either all-D or all-L octamers,[2] their capabilities in condensed-phase synthesis were investigated.[3] The preference of octamer formation for protonated oligomers[1] was found to be paralleled by their sodiated counterparts.[4] In addition, the remarkable preference of the monoprotonated serine octamer for homochirality[2] can be turned into a preference for heterochirality on addition of a second proton.[5] Only recently, halide anion binding clusters, i.e., negatively charged octamers[6] and nanometer-scale serine clusters generated by sonic spray ionization,[7] have enjoyed scientific interest. In parallel, several experimental and computational methods have been employed to elucidate the structure of the protonated octamer in the gas phase. The existence of serine dimers as building blocks was revealed from collision-induced dissociation (CID) experiments.[1,2,9] Both neutral−neutral and zwitterion−zwitterion dimers have been suggested, together with various all-zwitterion octamer clusters. The latter have been postulated, e.g., on the basis of ion-mobility measurements[7−9] and quantum-chemical calculations.[9] Interestingly, these ion-mobility experiments revealed only one isomer of the protonated serine octamer whereas two could be observed in H/D exchange experiments.[2] Even more interesting is that the slower-exchanging isomer (named A)[2] was found to form from homochiral serine only, whereas the faster-exchanging one (named B)[2] could also be obtained from a racemic mixture.[2] However, despite all of this experimental and computational evidence, the structure of $(\text{serine})_8\text{H}^+$ has still not been determined uniquely.[10]

In this study, we report the structural elucidation of both observed isomers of the protonated serine octamer from kinetic measurements of hydrogen/deuterium (H/D) exchange in the gas phase. This technique has already been applied to other amino acid clusters[11,12] and even peptides[13,14] and shall be laid out here in brief only. The protonated serine octamer, $C_{24}H_{57}N_8O_{24}^+$, is subjected to H/D exchange. All of its 33 labile hydrogen atoms undergo exchange, and the abundances of the species $C_{24}H_{57}N_8O_{24}^+$ (D_0 for short, no exchange) through $C_{24}H_{24}D_{33}N_8O_{24}^+$ (D_{33}, complete exchange) are monitored as

---

* To whom correspondence should be addressed. Telephone: +972-2-658 5866. Fax: +972-2-652 2472. E-mail: chavalu@vms.huji.ac.il.

[†] Dedicated to Professor Tom Baer on the occasion of his 65th birthday, in admiration of his outstanding contributions to the understanding of the physical chemistry of gas-phase ions through the elegant technique of photoelectron photoion coincidence (PEPICO).

10.1021/jp0451344 CCC: $30.25

a function of time. These experimental data are fitted to a given kinetic model. The model giving the best fit indicated by the best error function value is the model of choice (see Experimental Section). The kinetic model, in turn, reflects the structure of the cluster as illustrated here for the serine monomer: In the gas phase, serine ($\mathit{H}OCH_2CH(N\mathit{H}_2)COO\mathit{H}$) is neutral, and the labile hydrogen atoms indicated by italics are equivalent in groups of 2 (NH_2), 1 (OH), and 1 (COOH). However, for serine aggregates of the hexamer and beyond, quantum-mechanical calculations[9] favor zwitterionic serine units ($\mathit{H}OCH_2CH(N\mathit{H}_3^+)$-$COO^-$) with the labile hydrogen atoms being equivalent in groups of 3 (NH_3^+) and 1 (OH). These differences in the number and sizes of groups of equivalent hydrogen atoms (2/1/1 vs 3/1) are the basis of the analysis.

Experimental Section

L-Serine (Sigma, St. Louis, MO; 99%) was used without further purification. Solutions of serine were made in H_2O/CH_3OH (50:50, 2.5% acetic acid). ND_3 and CH_3OD were also from Sigma/Aldrich, with a stated isotopic purity that exceeds 99.5 atom % D.

Flow-Tube Experiments. The electrospray ionization/fast flow apparatus consists of an electrospray source connected directly to a flow tube. A neutral reagent is introduced into the flow tube through a ring inlet. Tylan mass flow controllers define the flow rate of the neutral reactant into the flow tube. The quadrupole mass analyzer (652601 ABB EXTREL, Pittsburgh, PA) is housed in a differentially pumped chamber that is separated from the flow tube by a nose cone (NC) skimmer with a 1.0 mm sampling orifice. An NC voltage is used for focusing ions into the analysis quadrupole. Helium buffer gas enters the flow tube at the upstream end through another Tylan flow controller. It is pumped through the tube by a Roots blower.

The electrospray ion source was designed as follows. A stainless steel capillary tube serves as the interface between the electrospray and the helium flow reactor. The entire assembly is inserted into the flow tube through an "O"-ring type vacuum fitting. The experiments to be described were carried out at a total flow velocity of ~7000 cm s^{-1} leading to a typical flow tube pressure of ~0.38 Torr and reaction periods of several ms. Ions were electrosprayed ~5 mm through ambient air into the grounded capillary tube from a nonconductive capillary made of 50 μm i.d. fused silica tubing biased at 5−6.5 kV dc. Then, an ~10 mM serine solution (see above for solvent) was delivered to the electrospray needle at a flow rate of 1.3 μL min^{-1} from a 1 mL syringe mounted on a model 100 KD Scientific Syringe Pump (kdScientific, Holliston, MA).

FT-ICR Experiments. Efficient formation of the serine octamer cluster was achieved by electrospraying a 1 mM serine solution (see above for solvent) at a flow rate of 300 nL/min into a home-built 9.4 T passively shielded ESI-Q-FT-ICR mass spectrometer[15] with a Chait-style atmosphere-to-vacuum interface with a heated metal capillary.[16] The ions were held in a focusing octopole, then transferred through a quadrupole mass filter in RF-only mode with no precursor ion isolation, and transferred to a linear octopole ion trap for 3 s of accumulation[17] before transfer to the open-ended cylindrical ICR trap for gas-phase H/D exchange. No precursor ion isolation was used for these experiments because it had been found that the faster exchanging isomer, B, is less stable than its A counterpart[2] and is diminished by any attempts to isolate the octamer,[18] one result of which is creation of the protonated serine dimer. For this exchange, deuterated methanol was admitted into the ICR cell via a pulsed valve connected to a variable leak valve.[19] The amount of gas delivered was set to reach a pressure of 5 × 10^{-7} Torr in the ICR cell, measured by a gauge located outside that cell. Following H/D exchange, a 150 s pumpdown delay removed the deuterating gas before excitation and detection of the ions. Ions were subjected to frequency sweep excitation (72−481 kHz at 150 Hz/μs) and broadband detection (512 kWord time-domain data). All aspects of the experiment were controlled by a modular ICR data acquisition system (MIDAS).[20] The reaction time periods were randomized and the experiment was run continuously, with the duration of the H/D exchange set by TcL scripting. The reported data are the sum of three scans.

Data Analysis. We analyzed kinetic data of H/D exchange by the development of a probabilistic algorithm,[12] which enabled us to discard the conventional and computationally demanding approach based on differential equations. It is described here in brief only: The probability that an H/D exchange of the *i*th hydrogen (proceeding at a rate of k_i) has not yet taken place at time t is $\neg p_i(t) = \exp(-k_i t)$ whereas the probability that it has taken place is $p_i(t) = 1 - \exp(-k_i t)$. Note that the sum of $p_i(t)$ and $\neg p_i(t)$ is exactly 1. For molecules with more than one labile hydrogen atom, mass spectrometry reveals the number of accomplished H/D exchanges but not their position. Thus, n out of N H/D exchanges are experimentally observed, and the probability P that they have taken place is the sum of the single-exchange probabilities. For instance, the probability that one H/D exchange out of three has taken place is $P_{1/3}(t) = p_1(t)\neg p_2(t)\neg p_3(t) + \neg p_1(t)p_2(t)\neg p_3(t) + \neg p_1(t)\neg p_2(t)p_3(t) = [1 - \exp(-k_1 t)]\exp(-k_2 t)\exp(-k_3 t) + \exp(-k_1 t)[1 - \exp(-k_2 t)]\exp(-k_3 t) + \exp(-k_1 t)\exp(-k_2 t)[1 - \exp(-k_3 t)]$. By minimizing the difference between the experimental data and the modeled probabilities $P_{n/N}(t)$, the site-specific H/D exchange rate constants k_i can be determined by nonlinear optimization.

Previously,[12] the implementation of this algorithm relied on bookkeeping of every structure between D_0 (no H/D exchange) and D_N (complete exchange). This was possible for the protonated arginine dimer with 15 labile hydrogen atoms.[12] However, for the protonated serine octamer with its 33 labile hydrogen atoms, 2^{33} or 8 589 934 592 structures per reaction period imposed memory requirements exceeding what is available on computers accessible to us. In addition, the individual treatment of every rate constant k_i did not allow for explicitly addressing symmetric structures with degenerate H/D exchange rate constants. Improving our algorithm to the stage reported here, however, meets these desires. Doing so, binomial coefficients come into play as shown here for the case of eight equivalent OH protons which is relevant for the serine octamer. The probabilities of 0, 1, 2, ..., 8 hydroxyl protons being replaced with a single probability of $p_{OH}(t)$ each, $P_{0/8}(t)$, $P_{1/8}(t)$, $P_{2/8}(t)$, ..., $P_{8/8}(t)$, are given by the successive terms of the binomial distribution

$$\binom{8}{0}\neg p_{OH}(t)^8,\ \binom{8}{1}\neg p_{OH}(t)^7 p_{OH}(t),\ \binom{8}{2}\neg p_{OH}(t)^6 p_{OH}(t)^2,\ ...,\\ \binom{8}{6}\neg p_{OH}(t)^2 p_{OH}(t)^6,\ \binom{8}{7}\neg p_{OH}(t) p_{OH}(t)^7,\ \binom{8}{8} p_{OH}(t)^8$$

Considering nonequivalent sites of H/D exchange, the replacements can be achieved by different combinations. For example, eight H/D exchanges in an octamer made up of eight neutral serine molecules can be achieved by eight OH replacements, with a probability of $p_{OH}(t)^8$, or by five out of eight OH replacements and three out of 16 NH_2 replacements, with a probability of

$$\binom{8}{5}\neg p_{OH}(t)^3 p_{OH}(t)^5 \cdot \binom{16}{3}\neg p_{NH_2}(t)^{13} p_{NH_2}(t)^3$$

etc. Eventually, the probabilities are summed for each set of structures with the same number of H/D exchanges to give the overall probability for that number of replacements.

Consequently, the implementation of the algorithm was modified as follows. (i) Degenerate rate constants are combined into a *block* of rate constants. There will be M blocks of rate constants with i being the blocks' running index. (ii) For a given block of rate constants, g_i is the size of that block or its rate constant's degree of degeneracy. (iii) With an additional running index j needed for bookkeeping, the equation for $P(n/N)$ is then

$$P(n/N) = \sum_{n_1=\max(0,n-N+g_1)}^{\min(n,g_1)} \sum_{n_2=\max(0,n-n_1-N+g_1+g_2)}^{\min(n-n_1,g_2)} \cdots \sum_{n_M=\max(0,n-\Sigma_{j=1}^{M-1}n_j-N+\Sigma_{j=1}^{M}g_j)}^{\min(n-\Sigma_{j=1}^{M-1}n_j,g_M)} \prod_{i=1}^{M} \binom{g_i}{n_i} p_i^{n_i} \neg\, p_i^{(g_i-n_i)} \tag{1}$$

whose last summation can be simplified because N equals $\Sigma_{j=1}^{M} g_j$:

$$P(n/N) = \sum_{n_1=\max(0,n-N+g_1)}^{\min(n,g_1)} \sum_{n_2=\max(0,n-n_1-N+g_1+g_2)}^{\min(n-n_1,g_2)} \cdots \sum_{n_M=\max(0,n-\Sigma_{j=1}^{M-1}n_j)}^{\min(n-\Sigma_{j=1}^{M-1}n_j,g_M)} \prod_{i=1}^{M} \binom{g_i}{n_i} p_i^{n_i} \neg\, p_i^{(g_i-n_i)} \tag{2}$$

During summation, the max functions account for the need to utilize all n substitutions for calculation of $P(n/N)$. Their min counterparts make sure that (i) the total number of substitutions does not exceed n and (ii) the respective block sizes g_i are not exceeded. Equations 1 and 2 apply to *all* systems including those with all $g_i = 1$ as well as to $n = 0$ and $n = N$. The modified algorithm was implemented in standard Fortran 95, compiled with the Intel Fortran Compiler for Linux, v. 6.0.0, and run on a Linux PC.

As mentioned in the Introduction, the structure determination is based on the deviation between experimental and modeled concentrations for species D_0 through D_{33}, for all reaction periods, as summarized in the error function. This error function ceases to improve when the model settings (number of ion populations and their respective labile hydrogen atom groupings) match the ion cluster's structure. For efficient use of CPU time, it is advisable to start with a maximum degeneracy of H/D exchange rate constants (for the system reported here, one population with 33 equivalent rate constants) and to subsequently ungroup labile hydrogen atoms according to plausible structures (for the system reported here, 32/1 for the single proton and 32 equivalent hydrogen atoms, 24/8/1 for an all-zwitterionic structure with a single proton, 16/8/8/1 for an all-neutral structure with a single proton, and so forth). In addition to reduced grouping, the number of ion populations may be increased as well. Each of the populations may have its own hydrogen atom grouping.

Results and Discussion

Flow-Tube Experiments. The bimodal H/D exchange reported by Cooks and co-workers[2] was matched by the experiments reported here for both ND_3 and CH_3OD. Figure 1 shows considerably faster exchange with ND_3 for one of the apparently two ion populations. Unfortunately, we were unable to follow on the flow tube the 33 H/D exchanges to completion. Therefore, a detailed kinetic analysis of the bimodal H/D exchange could not be undertaken.

However, it was possible to determine the sum of all exchange reaction rate constants as a real second-order rate constant from a pseudo first-order semilogarithmic decay plot of the reactant ion. The value obtained for the reaction of $(\text{serine})_8H^+$ with CH_3OD was 3.51×10^{-11} cm^3 molecule^{-1} s^{-1} which was used in connection with the kinetic analysis of the FT-ICR data (see below) to determine the individual second-order rate constants.

FT-ICR Experiments. As for the flow-tube experiments, two populations of the protonated serine octamer were observed in the FT-ICR experiments. With the FT-ICR experiments we are able to follow all 33 H/D exchanges for both populations. Again, this bimodal behavior is in agreement with previous results.[2] For clarity, we follow the established nomenclature:[2] population A exchanges its labile hydrogen atoms more slowly than population B (see Figure 2).

With inclusion of the initial concentrations of both populations into the search for the best-fitting model, populations A and B were found to be generated in a ratio of 75:20 and the sum of their H/D exchange rate constants to have a ratio of 1:9. Population A was found to undergo 33 equivalent H/D exchange reactions whereas population B showed groups of 16, 8, 8, and 1 equivalent exchange reactions with a rate constant ratio of 1:2:2:16 (see below for more details). Further sophistication of the model (i.e., reduction of symmetry) resulted in a minor improvement of fit that was not judged to be significant. Neither did the introduction of a third population, C. Thus, we concluded that the two-population approach is adequate within the experimental error both with respect to the number of populations and with respect to their possible but not observed interconversion. Experimental and modeled data are shown in Figures 3 and 4. The bimodal behavior is reproduced nicely. For reaction periods greater than 360 s, the fit is not as good as at shorter periods because only three species account for more than 60% of the total ion abundance. These species, however, appear only late in the experiment, and thus, their weight in the modeling is rather small.

With the help of the sum of all second-order rate constants determined in the flow-tube experiments (see above), the individual pseudo-first-order rate constants were converted into individual second-order rate constants. In principle, ICR experiments could also reveal second-order rate constants. However, exact determination of the deuterating gas pressure inside the ICR cell is problematic, especially if the pressure gauge is placed outside the ICR cell.[21] For the protonated serine octamer, the pseudo-first-order rate constant for population A was 0.61×10^{-2} s^{-1} (33×), leading to a sum of the 33 rate constants, $\Sigma(33k) = 0.20$ s^{-1}. For population B, the pseudo-first-order rate constants were 0.29×10^{-1} s^{-1} (16×), 0.58×10^{-1} s^{-1} (8×), 0.58×10^{-1} s^{-1} (8×), and 0.46 s^{-1} (1×) ($\rightarrow \Sigma(33k) = 1.86$ s^{-1}), respectively. Although the two 8-fold rate constants are very close in magnitude, unifying them in a 16/16/1 model caused the error function to become significantly worse. Consequently, we stayed with the 16/8/8/1 model of degeneracy. From the data just given, an overall reaction rate constant for populations A and B of 0.522 s^{-1} (which is in very good agreement with the value of 0.487 s^{-1}, derived as a pseudo-first-order rate constant from the consumption of D_0) corresponds to the overall rate constant of 3.51×10^{-11} cm^3 molecule^{-1} s^{-1} observed in our flow tube experiments. This value leads to a calculated CH_3OD

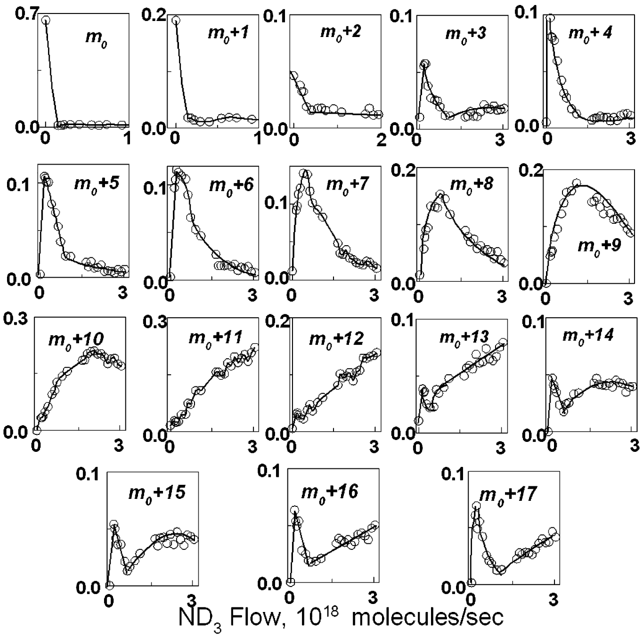

Figure 1. Relative abundance vs ND_3 flow rate in molecules s^{-1} for the unexchanged ion $(serine)_8H^+$, m_0 and for the various indicated cations for 17 consecutive exchanges (out of the 33 possible ones) in the flow tube reaction of $(serine)_8H^+$ with ND_3. Reaction period is 11.8 ms; helium carrier gas flow = 7.1 L min^{-1}; flow tube pressure = 0.377 Torr; maximum ND_3 concentration at the highest flow rate is ~1 × 10^{13} molecules cm^{-3}. The open circles are experimental, the continuous lines serve to lead the eye. (The data were not deconvolved to eliminate the isotopic distribution). The bimodal exchange kinetics can clearly be seen, particularly for ions $m_0 + 13$ through $m_0 + 17$.

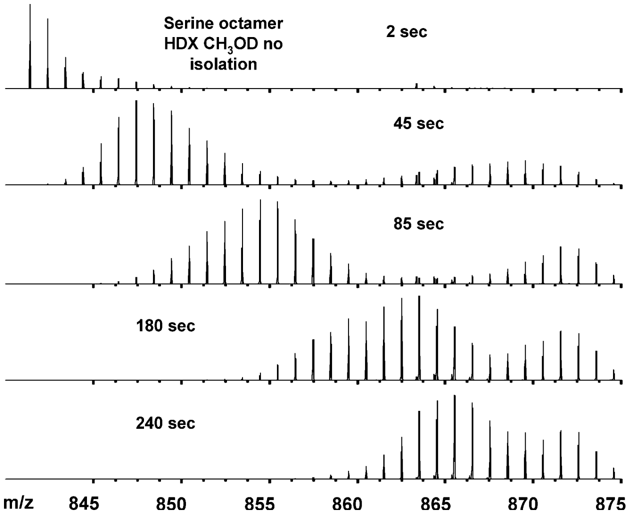

Figure 2. H/D exchange of the protonated serine octamer observed in an FT-ICR experiment at a CH_3OD pressure of 4.6×10^{-7} Torr. The two populations, A and B, become clearly separated.

density of 1.49×10^{10} molecules cm^{-3} and a calculated CH_3OD pressure of 4.6×10^{-7} Torr in the FT-ICR experiment. The calculated density allows extraction of the individual second-order rate constants. The rate constants deduced are as follows. (a) Population A: 33 equal rate constants, 4.10×10^{-13} cm^3 $molecule^{-1}$ s^{-1}, each ($\rightarrow\Sigma(33k) = 1.35 \times 10^{-11}$ cm^3 $molecule^{-1}$ s^{-1} which is in excellent agreement with the value, 1.4×10^{-11} cm^3 $molecule^{-1}$ s^{-1}, of the first overall H/D exchange rate of population A[22]). (b) Population B: 1.94×10^{-12} cm^3 $molecule^{-1}$ s^{-1} (16×), 3.92×10^{-12} cm^3 $molecule^{-1}$ s^{-1} (8×), 3.93×10^{-12} cm^3 $molecule^{-1}$ s^{-1} (8×), and 3.10×10^{-11} cm^3 $molecule^{-1}$ s^{-1} (1×) ($\rightarrow\Sigma(33k) = 1.25 \times 10^{-10}$ cm^3 $molecule^{-1}$ s^{-1}).

Structure of the Protonated Octamer Cluster. Before discussing the ion structures of populations A and B, we need to address the apparently contradictory result of ion mobility experiments.[7−9] In these experiments, only one population with a collisional cross section of about 190 Å^2 (187 Å^2, ref 9; 191 Å^2, ref 8; 190 Å^2, ref 7) was observed, whereas a second isomer could not be detected. The same was observed in a recent H/D exchange study of $(serine)_8H^+$.[22] Ion mobility and H/D exchange experiments, however, may lead to different results as observed for ubiquitin. In its 12-fold protonated state, this peptide shows two populations in H/D exchange experiments[23] but only one in ion mobility experiments,[24] as attributed to nearly identical cross sections.[25] For H/D exchange experiments, on the other hand, previous observations[2,18] and this study explain the seemingly contradictory results[22] easily: the ions of population B were found to be quite unstable toward collisions whereas the agreement in the first overall H/D exchange rate constant for population A is excellent (see the FT-ICR section above). Attempts to isolate the D_0 ion, $m/z = 841$, by either quadrupolar or SWIFT excitation of the unwanted ^{13}C- and ^{15}N-containing species, decreased the signal magnitude for population B significantly. Nonetheless, population B did not vanish completely (see Figure 5), thus not breaking down the bimodal kinetic scheme into a unimodal one but just reducing the signal-to-noise ratio of ion population B. Consequently, no attempts were undertaken to isolate $m/z = 841$ but the proper deconvolution of overlapping isotopic peaks was applied.

Regarding ion structures, the rate constant groupings for population A (the slower exchanging one) indicated the exclusive presence of zwitterion−zwitterion serine units, whereas for population B (the faster exchanging one), neutral−neutral serine dimers are the building blocks. These assignments are consistent with experimental results obtained by independent techniques and add one more piece of evidence to a self-consistent picture: population A undergoes slower H/D exchange than population B. The slow exchange and the 33 equivalent rate constants were originally attributed to the deuterating agent entering a central cavity of the compact cluster in the rate-determining step.[18] However, the following explanation involving an intracluster exchange mechanism is more plausible: COO^- groups on the outer surface of the compact cluster get deuterated and subsequently distribute the D atoms via the relay mechanism[26,27] over the entire cluster. This mechanism is consistent with the one observed for H/D exchange of zwitterionic $(arg)_2H^+$ (ref 28) and explains why 33 equal rate constants were found instead of the 24/8/1 grouping anticipated for an all-zwitterionic structure. A compact structure had already been found in ion mobility experiments, revealing a small collision cross section of about 190 Å^2 (refs 7−9), which, in turn, requires zwitterion−zwitterion dimers to build up the octamer.[9] The stronger zwitterion−zwitterion interactions that cause the more compact structure also give rise to the larger ion stability toward collisonal activation.[2,18] Population B, in contrast, undergoes faster H/D exchange, indicating a more open structure with easier access to the sites of proton exchange. Compared to population A, this open structure suggests neutral−neutral serine dimers rather than zwitterion−zwitterion dimers making up the octamer. In addition, equivalent hydrogens in groups of 16, 8, 8, and 1 indicate the presence of eight neutral serines: 16 amino hydrogens, eight carboxylic hydrogens, eight hydroxyl hydrogens, and one extra proton for the cluster charge. The more open (in other words:

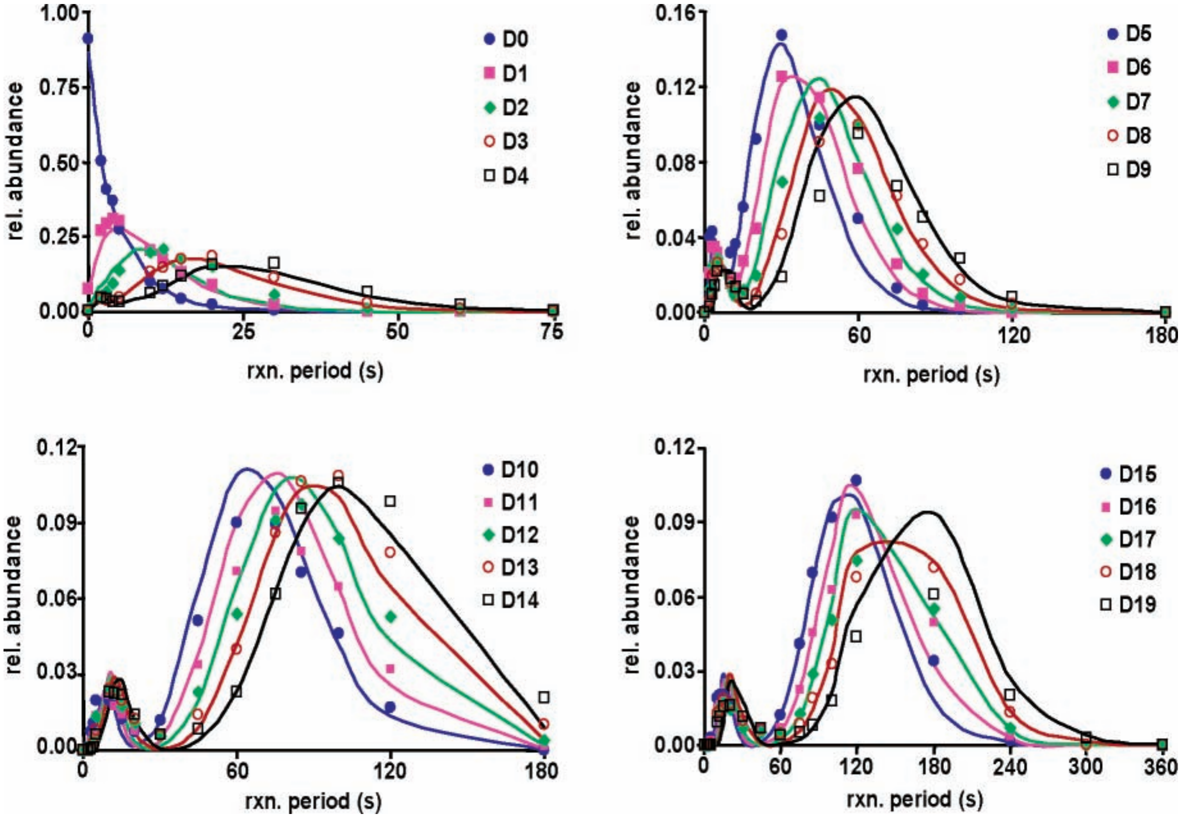

Figure 3. Isotopically deconvoluted experimental data (symbols) and modeled data (lines) for the H/D exchange of the protonated serine octamer observed in an FT-ICR experiment at a CH_3OD pressure of 4.6×10^{-7} Torr.

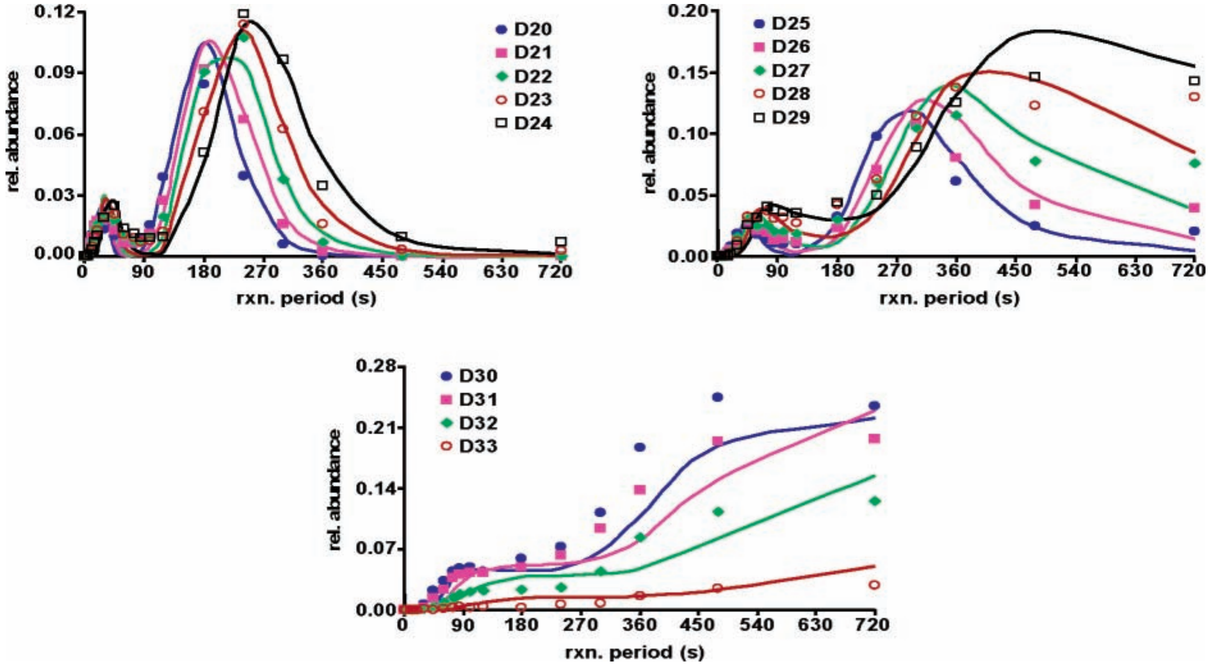

Figure 4. Isotopically deconvoluted experimental data (symbols) and modeled data (lines) for the H/D exchange of the protonated serine octamer observed in an FT-ICR experiment at a CH_3OD pressure of 4.6×10^{-7} Torr. For reaction periods greater than 360 s, the fit is not as good as before (see text for details).

less bound) structure is more susceptible to collision-induced dissociation (but nonetheless stable toward collisions with the deuterating agent) as found both previously[2,18] and in this work for attempts to isolate the D_0 species. Notably, the more stable ions of population A are formed from enantiomerically pure serine solutions only, whereas their B counterparts may be obtained from both enantiomerically pure and racemic solutions.[2] Thus, it appears that only the homochiral assembly of eight serine molecules is capable of forming a highly organized cluster which is stabilized by a multitude of strong intermolecular ion–ion interactions.

Conclusions

In this paper, we have investigated the H/D exchange kinetics of the protonated serine octamer. We observed the bimodal

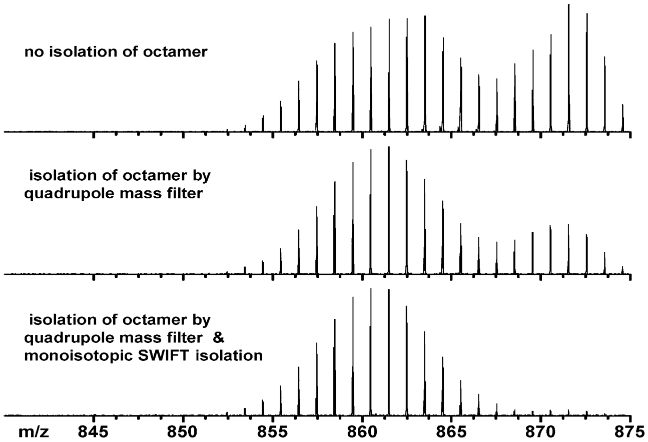

Figure 5. Decreased signal magnitude for population B after attempts to isolate the parent ion, $m/z = 841$, as compared to the original signal magnitude, observed in the absence of isolation attempts.

behavior previously reported[2] but not detected in ion-mobility experiments.[7−9] Improving our previously introduced probabilistic approach,[12] we were able to determine the H/D exchange rate constants. On the basis of their equivalence in groups of identical rate constants, we deduced the structures of both ion populations. To the slower exchanging population A we assigned an all-zwitterionic structure and an all-neutral structure to the faster exchanging population B. Population A is more stable toward collision-induced activation than population B. All of these findings are consistent with previous experimental results, thus comprising a self-consistent picture of the protonated serine octamer and its gas-phase properties.

Acknowledgment. Financial Support by the U.S.-Israel Binational Science Foundation (BSF) under Grant No. 2000026, the National Science Foundation (NSF) National High Field FT-ICR Facility under Grant No. CHE-99-09502, Florida State University, and the National High Magnetic Field Laboratory in Tallahassee, FL, are gratefully acknowledged. The Farkas-Center is supported by the Minerva Gesellschaft für die Forschung GmbH, München, Germany. U.M. and C.L. wish to thank the European Cluster Cooling Network (Grant No. HPRN-CT-2000-00026) for financial support and Prof. Ya'acov Ritov for his friendly help with the deconvolution. The authors wish to thank Professor R. Graham Cooks for making results of his group available prior to publication as well as for stimulating discussions.

References and Notes

(1) Cooks, R. G.; Zhang, D.; Koch, K. J.; Gozzo, F. C.; Eberlin, M. N. *Anal. Chem.* **2001**, *73*, 3646−3655.

(2) Takats, Z.; Nanita, S. C.; Schlosser, G.; Vekey, K.; Cooks, R. G. *Anal. Chem.* **2003**, *75*, 6147−6154.

(3) Takats, Z.; Nanita, S. C.; Cooks, R. G. *Angew. Chem.* **2003**, *115*, 3645−3647; *Angew. Chem., Int. Ed.* **2003**, *42*, 3521−3523.

(4) Kunimura, M.; Sakamoto, S.; Yamaguchi, K. *Org. Lett.* **2002**, *4*, 347−350.

(5) Julian, R. R.; Myung, S.; Clemmer, D. E. *J. Am. Chem. Soc.* **2004**, *126*, 4110−4111.

(6) Nanita, S. C.; Cooks, R. G. Submitted.

(7) Myung, S.; Julian, R. R.; Nanita, S. C.; Cooks, R. G.; Clemmer, D. E. *J. Phys. Chem. B* **2004**, *108*, 6105−6111.

(8) Counterman, A. E.; Clemmer, D. E. *J. Phys. Chem. B* **2001**, *105*, 8092−8096.

(9) Julian, R. R.; Hodyss, R.; Kinnear, B.; Jarrold, M. F.; Beauchamp, J. L. *J. Phys. Chem. B* **2002**, *106*, 1219−1228.

(10) Schalley, C. A.; Weis, P. *Int. J. Mass Spectrom.* **2002**, *221*, 9−19.

(11) Geller, O.; Lifshitz, C. *Int. J. Mass Spectrom.* **2003**, *227*, 77−85.

(12) Reuben, B. G.; Ritov, Y.; Geller, O.; McFarland, M. A.; Marshall, A. G.; Lifshitz, C. *Chem. Phys. Lett.* **2003**, *380*, 88−94.

(13) Beauchamp, J. L. H/D Exchange Reactions in Biological Molecules in the Gas Phase. In *The Encyclopedia of Mass Spectrometry*; Armentrout, P. B., Gross, M. L., Caprioli, R., Eds.; Elsevier: San Diego, CA, 2003; Vol. 1, Chapter 13.

(14) Cox, H. A.; Julian, R. R.; Lee, S.-W.; Beauchamp, J. L. *J. Am. Chem. Soc.* **2004**, *126*, 6485−6490.

(15) Senko, M. W.; Hendrickson, C. L.; PasaTolic, L.; Marto, J. A.; White, F. M.; Guan, S. H.; Marshall, A. G. *Rapid Commun. Mass Spectrom.* **1996**, *10*, 1824−1828.

(16) Chowdhury, S. K.; Katta, V.; Chait, B. T. *Rapid Commun. Mass Spectrom.* **1990**, *4*, 81−87.

(17) Hendrickson, C. L.; Quinn, J. P.; Emmett, M. R.; Marshall, A. G. Mass-Selective External Ion Accumulation for Fourier Transform Ion Cyclotron Resonance Mass Spectrometry. Presented at the 49th ASMS Conference on Mass Spectrometry and Allied Topics; Chicago, IL, 2001.

(18) Mazurek, U.; McFarland, M. A.; Marshall, A. G.; Lifshitz, C. *Eur. J. Mass Spectrom.* **2004**, *in press.*

(19) Jiao, C. Q.; Ranatunga, D. R. A.; Vaughn, W. E.; Freiser, B. S. *J. Am. Soc. Mass Spectrom.* **1996**, *7*, 118−122.

(20) Senko, M. W.; Canterbury, J. D.; Guan, S. H.; Marshall, A. G. *Rapid Commun. Mass Spectrom.* **1996**, *10*, 1839−1844.

(21) He, F.; Marshall, A. G.; Freitas, M. A. *J. Phys. Chem. B* **2001**, *105*, 2244−2249.

(22) Gronert, S.; O'Hair, R. A. J.; Fagin, A. E. *Chem. Commun.* **2004**, 1944−1945.

(23) Freitas, M. A.; Hendrickson, C. L.; Emmett, M. R.; Marshall, A. G. *Int. J. Mass Spectrom.* **1999**, *185/186/187*, 565−575.

(24) Valentine, S. J.; Counterman, A. E.; Clemmer, D. E. *J. Am. Soc. Mass Spectrom.* **1997**, *8*, 954−961.

(25) Purves, R. W.; Barnett, D. A.; Ells, B.; Guevremont, R. *J. Am. Soc. Mass Spectrom.* **2000**, *11*, 738−745.

(26) Campbell, S.; Rodgers, M. T.; Marzluff, E. M.; Beauchamp, J. L. *J. Am. Chem. Soc.* **1995**, *117*, 12840−12854.

(27) Green, M. K.; Lebrilla, C. B. *Mass Spectrom. Rev.* **1996**, *16*, 53−71.

(28) Geller, O.; Lifshitz, C. *J. Phys. Chem. A* **2003**, *107*, 5654−5659.